Clays and Clay Minerals, Vol. 43, No. 4, 438–445, 1995.

NATURE OF STRUCTURAL DISORDER IN NATURAL KAOLINITES: A NEW MODEL BASED ON COMPUTER SIMULATION OF POWDER DIFFRACTION DATA AND ELECTROSTATIC ENERGY CALCULATION

G. ARTIOLI,[1] M. BELLOTTO,[2] A. GUALTIERI[3] AND A. PAVESE[1]

[1] Università di Milano, Dipartimento di Scienze della Terra, I-20133 Milano, Italy

[2] CISE tecnologie innovative, I-20119 Segrate, Italy

[3] Università di Modena, Dipartimento di Scienze della Terra, I-41100 Modena, Italy

Abstract—A new model for the description of the structural disorder in natural kaolinite materials is proposed, based on the stacking of two 1:1 layers and their enantiomorphs, and encompassing previously proposed models. The layers, where randomly stacked along the c axis (using probabilistic functions nested in recursive algorithms), correctly describe the observed powder diffraction patterns of natural kaolinites with any density of structural faults. The proposed model was evaluated using electrostatic energy calculations against earlier models of disorder based on layer shift, layer rotation, statistical occupancy of the Al octahedra, or enantiomorphic layers. The present 4-layer model has a minimum of potential energy with respect to the previous models. As expected, the fully ordered triclinic structure of kaolinite possesses the absolute minimum of potential energy.

Key Words—Energy calculation, Kaolinite, Layer disorder, XRPD simulation.

INTRODUCTION

At present (a) there is no general model to describe the structure disorder in kaolinite, (b) the widely used empirical disorder indices, such as the Hinckley index, bear little relationship to the structural description of stacking disorder, and (c) proposed models of stacking disorder have not been compared with electrostatic energy calculations. These latter calculations were limited to the understanding of the hydroxyl crystal chemistry and bonding in the fully ordered structure (Giese 1982, Collins and Catlow, 1991, Bleam 1993).

We present here the results of computer simulations of X-ray diffraction powder patterns of kaolinites, using a general recursive algorithm applied to a new structural model of the stacking disorder. The simulations are compared to experimental powder diffraction patterns of natural kaolinites, and are shown to describe correctly the diffraction profiles of kaolinites with widely different fault densities. The technique is based on a rigorous recursion model, and it is of simple and general application. The proposed structure model is supported by the results of energy calculations.

Kaolinite, $Al_2Si_2O_5(OH)_4$, is a dioctahedral 1:1 layer aluminosilicate (Bailey 1980, Giese 1991), with one sheet composed of tetrahedrally coordinated Si and one sheet of octahedrally coordinated Al, with only $\frac{2}{3}$ of the octahedra being occupied in an ordered or a statistical way. The 1:1 layer has a triclinic distortion, due to the atom relaxation around the vacant aluminum site (usually denoted as the B-site). The non-hydrogen atom positions obey lattice C-centering (Adams 1983, Suitch and Young 1983, Thompson and Withers 1987, Young and Hewat 1988, Bish and Von Dreele 1989, Collins and Catlow 1991, Bish 1993) with space group C1 for the unit triclinic layer. Atomic positions from Bish and Von Dreele (1989) were used, yielding a simulated X-ray powder pattern in perfect agreement with the most ordered known natural kaolinite, the sample from Keokuk, Iowa (Bish and Von Dreele 1989, Giese 1991, Bish 1993).

EXPERIMENTAL PROCEDURES

X-ray powder pattern: experimental profiles

Two natural kaolinite samples were selected because of their purity and because they represent well-ordered and poorly-ordered materials. The "ordered" kaolinite (KAOSAR) is from a 6 cm thick vein of hydrothermally recrystallized pure kaolinite from Casa Locchera, Nuraghe Mandras sas Ebbas, Sardinia, Italy (Coulon 1971). It is purer and more "ordered" than Clay Minerals Society Standard KGa-1 (Van Olphen and Fripiat 1979). The "poorly-ordered" specimen is the Clay Minerals Society Standard KGa-2 from Warren County, Georgia (Van Olphen and Fripiat 1979). It contains minor amounts of anatase.

The two powder specimens were analyzed for grain-size distribution using laser diffraction (Fritsch Particle Size Analysette 22). Both samples have a bimodal distribution, with grain-size peak maxima at 5 and 15 μm. The two powder samples were then side-loaded in an aluminum holder, and the X-ray powder diffraction data (Figure 1) were collected on a Philips goniometer using graphite monochromatized CuKα radiation, a Bragg-Brentano parafocussing geometry, a step/scan

mode with 0.02 °2θ steps, a counting time of 10 sec/step, and a 5–50 °2θ range.

X-ray powder pattern: simulated profiles

The program DIFFaX (Treacy *et al* 1991) is based on a rigorous recursion method for the generation of random stacking sequences modelling the presence of planar faults. The method exploits the self-similar stacking sequences occurring in a non-deterministic layer stack, so that the recursive relations between the average interference terms from a statistical crystal are solved as a set of simultanous equations. The method is formally equivalent to previous mathematical treatments such as the Hendricks-Teller matrix formulation and its developments (Hendricks and Teller 1942, Allegra 1964, Kakinoki and Komura 1965), the series summation formula (Cowley 1976), or Michalski's recurrence relations between average phase factors (Michalsky 1988). The program allows the calculation of the incoherent sum of scattered intensities from a finite ensemble of layers stacked along a direction, and the stacking can be described in terms of the probability of any sequence of layers. The full description of disorder in each simulation implies a square probability matrix of order n (with n equal to the number of crystallographically distinct layers), where each element M_{ij} refers to the probability of stacking layer j over layer i in the sequence. From the hierarchical tree of probabilities due to the nested recursion we can compute the probability (P_l) of finding a single layer in the crystal ensemble, and the total density of stacking faults in the sequence (P_d).

As an example, for a crystal composed of three layers (H, K, and L) having a probability matrix

$$M = \begin{array}{c} \\ H \\ K \\ L \end{array} \begin{array}{c} \begin{array}{ccc} H & K & L \end{array} \\ \begin{pmatrix} 0.50 & 0.25 & 0.25 \\ 0.25 & 0.50 & 0.25 \\ 0.25 & 0.25 & 0.50 \end{pmatrix} \end{array}$$

we have that layer H has probabilities $M_{HH} = 0.50$, $M_{HK} = 0.25$, and $M_{HL} = 0.25$, of being followed by an H, K, or L layer respectively. Furthermore, in the final ensemble of crystallites we will find statistically each layer with probabilities close to $P_H = 0.33$, $P_K = 0.33$, and $P_L = 0.33$, and if we refer to the unfaulted crystal as having $P_d = 0.0$, then we have in our sample a total of $P_d = 0.50$ of disordered sequences.

For kaolinite, we interpret the statistical probability indicated by each matrix element as related to the crystallochemical probability of faulting in the structure, so that the M_{ij} values have direct control on the final density of planar faults in the crystal. Therefore, by gauging the matrix elements, we can control the interaction probability between any two layers in the structure, and at the same time evaluate the final density of stacking faults in the crystalline ensemble.

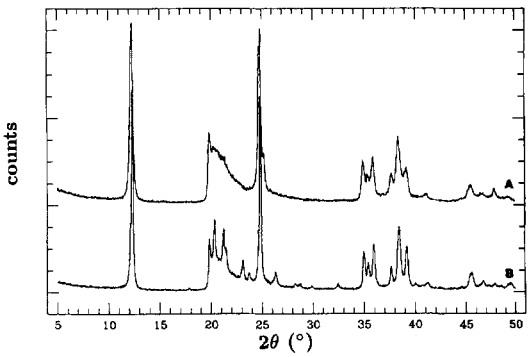

Figure 1. Experimental X-ray powder diffraction patterns for the two natural reference kaolinite samples: (A) poorly crystallized kaolinite KGa-2 from Warren County, Georgia, United States; and (B) well-crystallized kaolinite from Nuraghe Mandras sas Ebbas, Sardinia, Italy. The profile a was shifted relative to the vertical axis, and vertical units refer to profile b.

To adapt the structure to this statistical treatment, the unit layer must be orthogonalized along the stacking direction, and the modified (i.e., shifted, rotated or enantiomorphic) layers must be defined crystallographically with the appropriate transformation matrices.

The computer simulation of kaolinite is developed in several steps. First, we describe the triclinic layer unit of kaolinite using z orthogonal to the ab plane to describe any layer stacking, shift or rotation easily. We then determine that the ordered structure is correctly described in the pseudo-monoclinic coordinate system, by comparing the diffraction profile from DIFFaX with other programs (Larson and Von Dreele 1993). All simulated diffraction patterns are in the range 5–50 °2θ, employ CuKα radiation, and utilize a pseudo-Voigt function to describe the intensity distribution of the Bragg peaks due to instrumental and sample effects.

We then introduce the simulation of structural disorder of kaolinite using previously described models (e.g., see Brindley 1980 and Drits and Tchoubar 1990). Classical models of stacking faults in kaolinite are based on $\pm$b/3 layer shifts (Plançon and Tchoubar 1975), $\pm$120° layer rotations (Plançon and Tchoubar 1976), or displacement of Al vacancies (Plançon and Tchoubar 1977b) over the three octahedral sites (labelled A, B, or C in the notation of Bailey 1963). Note that the vacant octahedral site in each layer is laying on the pseudo-mirror plane, and it is referred here as the B-site; the layer with the A and C positions occupied and the B position vacant is referred to as the B-layer. We calculated the pattern relative to each simple model, and for each model we applied different densities of stacking faults. Figure 2 shows the resulting patterns for the linear shift model. Patterns 2a, 2b, and 2c refer to P_d of 0.67, 0.50 and 0.30, respectively, with equal contribution from 1:1 layers displaced of b/3 and 2b/

https://doi.org/10.1346/CCMN.1995.0430407 Published online by Cambridge University Press

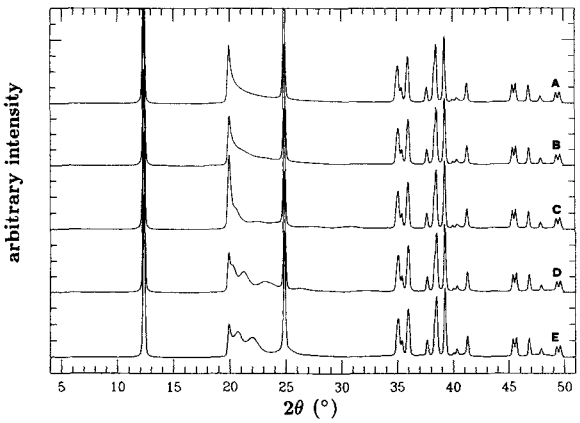

Figure 2. Simulated X-ray powder diffraction profiles for kaolinite assuming the linear translational model. Details of the models for patterns 2a–2e are listed in Table 1. Vertical axis is in arbitrary units.

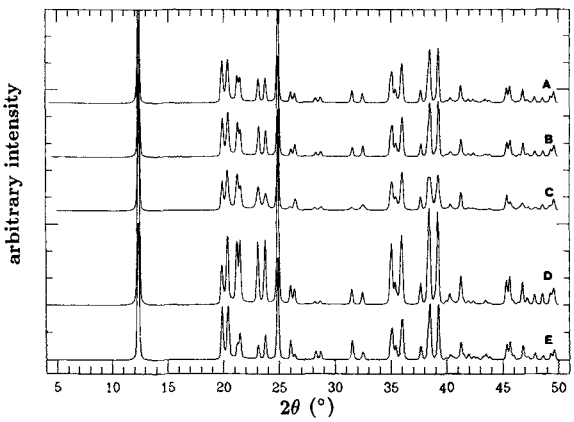

Figure 4. Simulated X-ray powder diffraction profiles for kaolinite assuming the Al vacancies displacement model. Details of the models for patterns 4a–4e are listed in Table 1. Vertical axis is in arbitrary units.

3. Patterns 2d and 2e have a total disorder of P_d = 0.50, and contain contributions from only b/3-displaced and only 2b/3-displaced layers, respectively. Figure 3 shows the patterns resulting from simulation of disorder due to layer rotation, and Figure 4 shows the patterns resulting from the displacement of Al vacancies in A-, B-, and C-layers. Table 1 lists the detailed model for each powder pattern simulation. More complex models of structure disorder are described also in the same Table, they are discussed below.

Our simulated patterns agree well with those of Plançon and Tchoubar (Plançon and Tchoubar 1977a, Plançon 1981, Drits and Tchoubar 1990), which are based on the matrix method (Kakinoki and Komura 1965). For example, our Figure 3d is identical to Figure 7 of Plançon and Tchoubar (1977b). There are, however, advantages in using DIFFaX. First, the scattering contribution is calculated for the whole spectrum, whereas their model involves a scattering contribution from select regions of reciprocal space. The scattering due to the basal (00l) planes is evident in our computed profiles, but absent in their spectra, and it must be added *a posteriori*. Moreover, the total density of stacking defects in the sample is readily evaluated from our stacking probability functions, whereas each of their fitted parameters has a different structural significance and depends on specific regions of the diffraction pattern (Plançon and Zacharie 1990). The main limitation of our technique for the direct characterization of natural samples is the present inability to minimize the discrepancies between observed and calculated powder profiles.

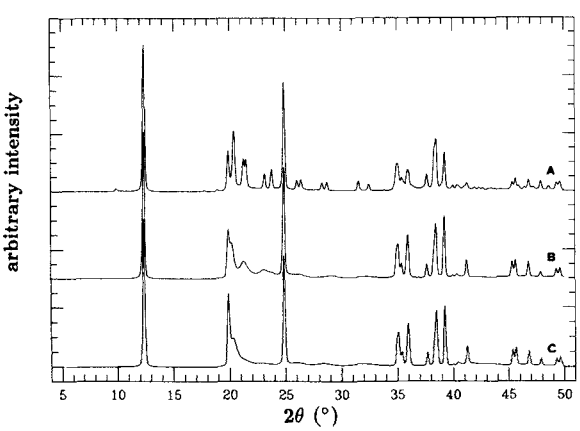

Figure 3. Simulated X-ray powder diffraction profiles for kaolinite assuming the rotational model. Details of the models for patterns 3a–3c are listed in Table 1. Vertical axis is in arbitrary units.

Electrostatic energy calculation: theory

Energy calculation for kaolinite in the past used semiempirical methods, treating the structure as an ideal ionic solid (see reviews by Giese 1982 and Bleam 1993) and were devoted to interlayer bonding and hydroxyl orientation in the structure. Hess and Saunders (1992), using the *ab initio* Hartree-Fock method to define hydroxyl positions, is one of the few quantum-mechanical calculations on layer silicates. We apply below purely electrostatic semiempirical potentials to the energy calculation of kaolinite, to compare the relative stability energies of the models proposed for the description of the stacking disorder.

We used the method of Collins and Catlow (1991), where the oxygen-hydrogen interaction in the hydroxyl groups is described by a Morse-type model and all the other interactions are treated by purely Coulombic potentials, making use of fractionary charges for the atoms of the hydroxyl groups, and of formal charges for other atoms. The reciprocal lattice sum is based on the

https://doi.org/10.1346/CCMN.1995.0430407 Published online by Cambridge University Press

Table 1. Probability matrix M and density of stacking faults P_d for the models of disorder in kaolinite.

Fig. n.*	M_{11}	M_{12}	M_{13}	M_{21}	M_{22}	M_{23}	M_{31}	M_{32}	M_{33}	P_d
Models with $\pm b/3$ translations l_1 = untranslated B-layer; l_2 = b/3 translated layer; l_3 = 2b/3 translated layer										
2a	0.33	0.33	0.33	0.33	0.33	0.33	0.33	0.33	0.33	0.67
2b	0.50	0.25	0.25	0.25	0.50	0.25	0.25	0.25	0.50	0.50
2c	0.70	0.15	0.15	0.15	0.70	0.15	0.15	0.15	0.70	0.30
2d	0.50	0.50	0.00	0.50	0.50	0.00	0.50	0.50	0.00	0.50
2e	0.50	0.00	0.50	0.50	0.00	0.50	0.50	0.00	0.50	0.50
Models with $\pm 120°$ rotations l_1 = B-layer; l_2 = 120° rotated layer; l_3 = 120° rotated layer										
3a	0.33	0.33	0.33	0.33	0.33	0.33	0.33	0.33	0.33	0.67
3b	0.50	0.25	0.25	0.25	0.50	0.25	0.25	0.25	0.50	0.50
3c	0.70	0.15	0.15	0.15	0.70	0.15	0.15	0.15	0.70	0.30
Models with disorder over the octahedral sites l_1 = B-layer; l_2 = C-layer; l_3 = A-layer										
4a	0.33	0.33	0.33	0.33	0.33	0.33	0.33	0.33	0.33	0.67
4b	0.50	0.25	0.25	0.25	0.50	0.25	0.25	0.25	0.50	0.50
4c	0.70	0.15	0.15	0.15	0.70	0.15	0.15	0.15	0.70	0.30
4d	0.50	0.50	0.00	0.50	0.50	0.00	0.50	0.50	0.00	0.50
4e	0.50	0.00	0.50	0.50	0.00	0.50	0.50	0.00	0.50	0.50
Models with enantiomorphic and C-layer l_1 = B-layer; l_2 = enantiomorphic layer; l_3 = C-layer										
5a	0.50	0.50	0.00	0.50	0.50	0.00	0.50	0.50	0.00	0.50
5b	0.33	0.33	0.33	0.66	0.33	0.00	0.66	0.00	0.33	0.67
5c	0.10	0.45	0.45	0.90	0.10	0.00	0.90	0.00	0.10	0.90

* The Figure n. refers to the graphical profile representation of each model.

Ewald method (Bertaut 1952). The hydroxyl orientations in each layer are fixed according to the results of Collins and Catlow (1991), and the coefficients of the interatomic potentials were used in the program ENE (Catti 1978) to obtain values for the total energy of the disordered structures.

Statistical sequences were approximated by super-cells having c′ = nc, where c is the 1:1 layer thickness. The integer n varies depending on the stacking sequence of the disorder model considered. The deterministic structural sequence defined for the energy calculations is not directly comparable to the statistical one produced by the recursive DIFFaX method, but the results are meaningful for a general comparison among the models. The transformation matrices used in the powder pattern simulation to generate the shifted, rotated, and enantiomorphic layers, originating from the 1:1 layer, were applied rigorously to define the super-cells of the energy calculations.

The results are listed in Table 2, reporting the super-cell and the energy values referred to single atoms for each model.

RESULTS AND DISCUSSION

Simulations of earlier models for kaolinite disorder

The simulations of the X-ray powder patterns resulting from the simple models of structural disorder (Figures 2–4) indicate that these are inadequate to describe the faulted nature of kaolinite materials. This was discussed earlier (Plançon and Tchoubar 1975, 1976, 1977b, Drits and Tchoubar 1990). These models were generally based on the idealized (undistorted) layer of kaolinite, and nearly all previous simulations considered only select regions of the profiles.

The present simulation of the profiles in the 2θ = 5–55° range, based on the triclinic distortion of the 1:1 layer, allows us to obtain detailed information about each model.

Clearly, from patterns 2d and 2e (Figure 2), b/3 and 2b/3 (or −b/3) shifts are not equivalent due to the different number of Al cations facing Si atoms in the next layer, even if they were considered as such in earlier models (Brindley and Robinson 1946, Brindley 1980). Furthermore, none of the modulations produced by the two models on the diffraction band in the angular range 20–24 °2θ (commonly referred to as the (02, 11) band) reflects the observed modulation of the diffraction patterns of natural samples. The inadequacy of the linear translational model was discussed on the basis of electrostatic arguments by Newnham (1961), Giese (1982), and Drits and Tchoubar (1990).

Also the simulations involving rotational disorder (Figure 3) clearly show that 120 and 240° rotations yield different stacking sequences if based on the triclinic layer. The simulated patterns involving rotational disorder are not appropriate to describe natural kaolinite, due to lattice misfit between adjacent layers

Table 2. Energy value renormalized to single atoms E_{ren} for the models of disorder of kaolinite.

Model	E_{ren}	n^*
Model with ordered B-layer		
l_1 = B-layer		
l_1 sequence	−29.41	1
Model with ±b/3 translations		
l_1 = untranslated B-layer; l_2 = b/3 translated layer; l_3 = 2b/3 translated layer		
l_1, l_2, l_3 sequence	−13.16	3
l_1, l_3, l_2 sequence	−19.11	3
Models with ±120° rotations		
l_1 = unrotated B-layer; l_2 = 120° rotated layer; l_3 = −120° rotated layer		
l_1, l_2, l_3 sequence	−24.67	3
l_1, l_3, l_2 sequence	−25.08	3
Models with statistical disorder over the octahedral sites		
l_1 = B-layer; l_2 = C-layer; l_3 = A-layer		
l_1, l_2, l_3 sequence	−28.23	3
l_1, l_2, l_3 sequence	−28.38	3
Models with enantiomorphic and C-layer		
l_1 = B-layer; l_2 = enantiomorphic layer; l_3 = C-layer		
l_1, l_2 sequence	−27.51	2
l_1, l_2, l_3 sequence	−28.01	3
l_1, l_3, l_2 sequence	−26.97	3
Improved models with enantiomorphic layers and C-layer		
l_1 = B-layer; l_2 = enantiomorphic B-layer; l_3 = C-layer; l_4 = enantiomorphic C-layer		
l_1, l_2, l_3, l_4 sequence	−28.68	4
l_1, l_3, l_4, l_2 sequence	−28.68	4

* The lattice c' of the super-cell (see text for details) is nc, where c is the layer thickness of the ordered kaolinite layer.

produced by rotation around the center of the pseudo-hexagonal ring of tetrahedra. The rotational model is strictly applicable only to idealized layers having hexagonal or ditrigonal symmetry, since 1:1 layers with triclinic distortions produce lattice incommensurability (Plançon and Tchoubar 1976, Drits and Tchoubar 1990).

The model involving fixed kaolinite layers with displacement of the Al vacancies over the octahedral sites, introduced by Plançon and Tchoubar (1977b) as a compromise between the two preceding models, has several problems. The model ignores layer relaxation around the vacant octahedral site, and Figure 4 clearly shows that the model does not account for the observed modulation of the (02,11) band even with a density of stacking defects as high as $P_d = 0.67$. This is particularly evident in the region around 21 °2θ, where all the simulations in Figure 4 show the well defined $(\bar{1}\bar{1}1)$ and $(\bar{1}11)$ doublet, which is not observed in defect-rich kaolinites. Interestingly, this model implies ordered sequences of dickite in the kaolinite crystallites, by incorporation of domains of B-, and C-layer alternation (Brindley 1980). Although this dickite-kaolinite intergrowth has found support from infra-red studies (Brindley *et al* 1986), the X-ray diffraction patterns based on this model do not account satisfactorily for the observed powder patterns of natural kaolinites (Drits and Tchoubar 1990). Furthermore, the model (Plançon and Tchoubar 1977a, Plançon 1981) is relatively unsensitive to the fine details of the observed powder spectra, since it produces the same simulated bands using different sets of stacking variables (Plançon and Tchoubar 1977b, Tchoubar *et al* 1982).

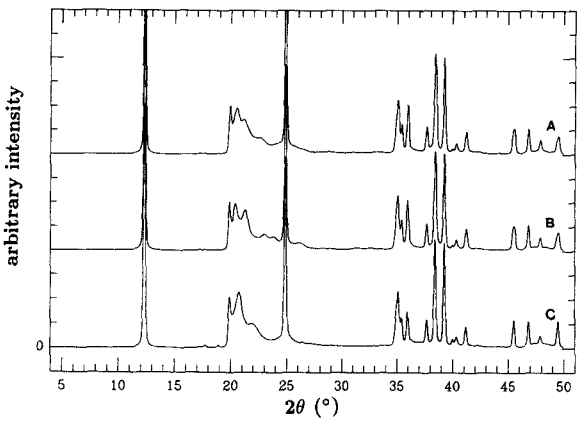

Figure 5. Simulated X-ray powder diffraction profiles for kaolinite assuming the models with enantiomorphic layers. Details of the models for patterns 5a–5c are listed in Table 1. Vertical axis is in arbitrary units.

The pseudo-mirror plane in the layer can result in a different kind of stacking fault, induced by the succession of two triclinic layers related by the mirror plane. The two layers are enantiomorphs of each other, and the stacking fault may be regarded as the intergrowth of left- and right-handed kaolinite forms. This model, introduced by Bookin *et al* (1989), produces only minor perturbations to the electrostatic energy interaction between layers, and produces the X-ray diffraction modulations in the (02, 11) band rather well. Figure 5a is based on the enantiomorphic model with a total density of $P_d = 0.50$ of stacking between the two layers. The enantiomorphic B-layer is obtained through 60° rotation of the (100)-reflected layer. As noted by Bookin *et al* (1989) these stacking faults have major effects on the (02, 11) diffraction band, but leave almost unaltered the Bragg peaks in the region 34–40 °2θ (commonly labelled the (20, 13) band), which in diffraction patterns of natural kaolinites is also affected by broadening and modulation effects. This is the reason for the insertion of stacking faults due to C-layers in the model formed by enantiomorphic layers (Bookin *et al* 1989). As noted previously, the effect on the diffraction pattern due to the additional C-layer approximates the effect due to ±b/3 shifts. This latter model is complex but applied with some success to the quantification of defects in natural kaolinites (Plançon *et al* 1989). This model is used in powder patterns 5b and 5c (Figure 5)

https://doi.org/10.1346/CCMN.1995.0430407 Published online by Cambridge University Press

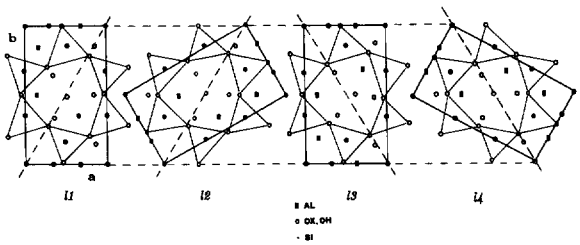

Figure 6. Structure diagram of the 4-layer models of disorder in kaolinite. The layers are horizontally translated for clarity, while in the actual model they are stacked so that the dashed cells share the same c stacking vector. The four layers are plotted with the true triclinic layer distortion: (l1) triclinic B-layer, (l2) enantiomorphic of the B-layer, (l3) triclinic C-layer, (l4) enantiomorphic of the C-layer.

by using total stacking densities of $P_d = 0.67$ and $P_d = 0.90$, respectively. The sequence, as originally proposed, has high probability of transitions between the normal B-layer and the enantiomorphic or the C-layer to simulate a total high density of faults, but at the same time it has low probability of transitions between two C-layers and of ordered B-C sequences, in order to eliminate the possibility of extensive domains of ordered kaolinite and/or dickite in the crystallites. This is the physical interpretation of the matrix coefficients we introduced for model 5c (Table 1).

Improved model for kaolinite disorder

As shown in Figure 5, the model for kaolinite disorder involving B-enantiomorphic and C-layers represents a remarkable improvement in the simulation of kaolinite diffraction patterns. The model also suggests that both the C-layer and its enantiomorph coexist. Since the succession of the B-layer and its enantiomorph is energetically reasonable, as discussed below, it follows that the succession of the C-layer and its enantiomorph may similarly exist. Moreover the stacking ordered sequences of B-enantiomorphic and C-enantiomorphic layers physically represent domains of "monoclinic" kaolinite, much like the ordered sequences of B-layers and C-layers.

The model we present is based on four structurally distinct layers (Figure 6). It makes it possible to simulate an ensemble of kaolinite crystallites with any total density of stacking defects. Furthermore, by varying the matrix probability coefficients, the physical significance of the statistical layer sequence may be controlled. For example, we might assume that the transitions between the B-layer and its enantiomorphic (or between the C-layer and its enantiomorphic) are more energetically favoured than the B-layer C-layer transitions. Thus, whenever a C-layer occurs, it should be followed by a B-layer rather than another C-layer, as discussed above. Some X-ray powder pattern simulations based on the 4-layer models are shown in Figure 7, with matrix coefficients relative to each profile and other relevant parameters listed in Table 3. Note that the model can adequately describe kaolinites with any density of defects: pattern 7e represents a defect-free material, and it is nearly identical with the observed diffraction pattern of the Keokuk kaolinite reported by Bish and Von Dreele (1989); patterns 7a–d show the effect produced by the decreasing amount of total stacking faults on the scattering profile. The Hinckley indices (Brindley 1980, Plançon *et al* 1988) calculated for these simulated patterns show that there is a near linear relationship between this empirical parameter for kaolinite "crystallinity" and the density of stacking faults in the structure, as evaluated from the probability matrix (Figure 8).

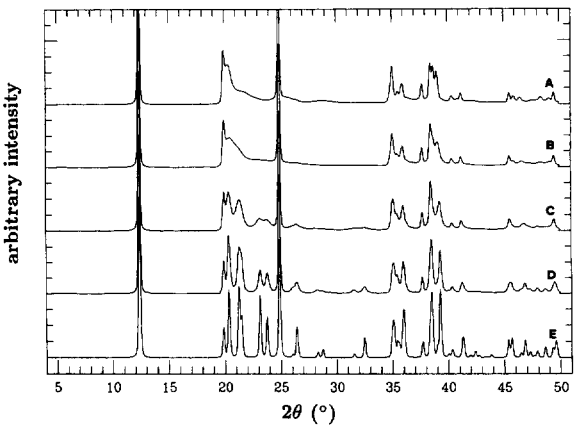

Figure 7. Simulated X-ray powder diffraction profiles for kaolinite assuming the 4-layer model. Details of the model for patterns 7a–7e are listed in Table 2. Vertical axis is in arbitrary units.

Note also that the intensity degradation is evident on every non-basal Bragg peak in the pattern, in agreement with the features of observed patterns, and the

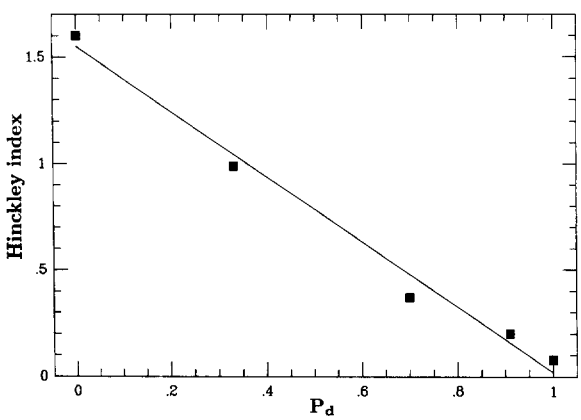

Figure 8. Correlation between the Hinckley index and the density of stacking faults (P_d) relative to the sequence of simulated X-ray powder patterns shown in Figure 7.

https://doi.org/10.1346/CCMN.1995.0430407 Published online by Cambridge University Press

Table 3. Probability matrix M and density of stacking faults P_d for the 4-layers improved model of disorder of kaolinite.

Fig. n.*	M_{11}	M_{12}	M_{13}	M_{14}	M_{21}	M_{22}	M_{23}	M_{24}	M_{31}	M_{32}	M_{33}	M_{34}	M_{41}	M_{42}	M_{43}	M_{44}	P_d
4-layers improved model																	
l_1 = B-layer; l_2 = enantiomorphic B-layer; l_3 = C-layer; l_4 = enantiomorphic C-layer.																	
7a	0.00	0.50	0.50	0.00	0.50	0.00	0.00	0.50	0.50	0.00	0.00	0.50	0.00	0.50	0.50	0.00	1.00
7b	0.33	0.33	0.33	0.00	0.33	0.33	0.00	0.33	0.33	0.00	0.33	0.33	0.00	0.33	0.33	0.33	0.67
7c	0.70	0.15	0.15	0.00	0.15	0.70	0.00	0.15	0.15	0.00	0.70	0.15	0.00	0.15	0.15	0.70	0.30
7d	0.91	0.05	0.04	0.00	0.05	0.91	0.00	0.04	0.04	0.00	0.91	0.05	0.00	0.04	0.05	0.91	0.09
7e	1.00	0.00	0.00	0.00	0.00	0.10	0.00	0.00	0.00	0.00	1.00	0.00	0.00	0.00	0.00	1.00	0.00

* The Figure n. refers to the graphical profile representation of each model.

broadening effects are not limited to selected portions of the profile. In addition to peak broadening, there is also a substantial background modulation which is proportional to the number of stacking defects. This is also evident in most observed X-ray patterns of kaolinites, and it is due to incoherent scattering. All fine features of the experimental patterns are satisfactorily simulated by the 4-layer model, especially the slight shifts of certain reflections (i.e., $(\bar{1}10)$ and $(\bar{1}\bar{1}1)$), which are critically dependent on the average lattice symmetry and on the relative amount of C- and C-enantiomorphic layers.

The models of disorder which best describe the KAOSAR and KGa-2 kaolinite samples were obtained by changing the layer stacking probabilities stepwise, and by comparing the profile agreement factors ($R_{wp} = (\Sigma w(I_o - I_c)^2)/(\Sigma w(Io)^2)$) between the observed and calculated profiles in the profile regions affected by disorder (19.5–25 °2θ, 34–42 °2θ, and 45–50 °2θ). The simulated profiles shown in Figure 9 yield $R_{wp} = 0.45$ and $R_{wp} = 0.49$ for KAOSAR and KGa-2 respectively. The densities of stacking defects derived from the probability matrix of the best-fit models are: $P_d = 0.14$ for KAOSAR and $P_d = 0.50$ for KGa-2.

The instrumental profile shape and the background functions have not been refined, and this is reflected in the high R_{wp} values. The agreement factors between the same observed profiles and the simulated patterns using the disorder models from the literature (including the earlier enantiomorphic model of Bookin *et al* 1989) produce values above 0.60.

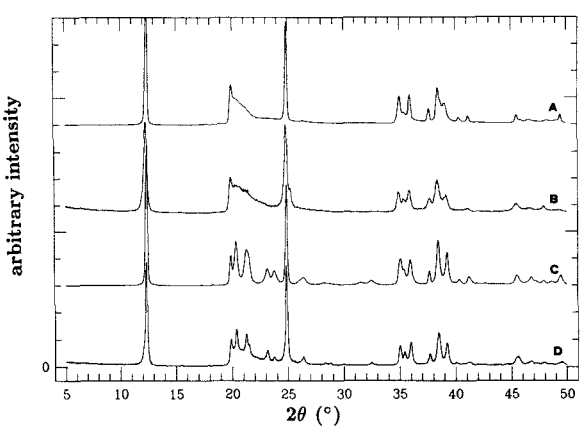

Figure 9. Comparison of simulated (A and C) and observed (B and D) powder diffraction patterns for the reference kaolinite samples of Figure 1.

Comparison of electrostatic energy calculations

A comparison of the normalized energy values in Table 2 shows that the ordered triclinic kaolinite structure is the more energetically stable. The fact that natural kaolinites commonly show a high degree of disorder clearly indicates that most samples are metastable with respect to the fully ordered structure.

Models with displacements of octahedral Al vacancies have inconsistencies relating to the lack of relaxation around the vacant sites, and the interatomic distances involve improperly distorted sites. Relaxation effects may result in significantly different energy values. The models involving shifts or rotations show significant deviation from the energy minimum and are less favoured models. Among the models containing enantiomorphic layers, the one with the 4-layer sequence shows the lower energy minimum. Calculations involving a 4-layer model with different sequences of the layers did not result in significant variations of the total energy. Thus the 4-layer models are energetically favoured with respect to any model of stacking disorder based on three kinds of layers.

SUMMARY

We introduce a model for structural disorder in kaolinite based on four crystallographically different unit layers. The model is supported by the results of electrostatic energy calculations. Using a recursive technique, the model successfully describes the scattering modulations observed in natural kaolinites having different densities of stacking defects.

The proposed model has several advantages: (a) it includes all previously proposed models of kaolinite disorder which have physical and crystallographic significance; (b) it is very flexible and allows description of different kinds of faulting at the same time, including enantiomorphic distortions and displacement of octahedral Al vacancies; (c) it reproduces the observed X-ray powder diffraction patterns of any natural ka-

olinite, from defect-free to highly-faulted materials; and (d) it allows a straighforward qualitative and quantitative interpretation of the total density of stacking faults in the crystallite ensemble.

ACKNOWLEDGMENTS

This work received support by Italian MURST and CNR. Part of this study was performed by Dr. A. Gualtieri during his doctorate work at the University of Modena. Thanks to Prof. M. Catti for making the program ENE available to us.

REFERENCES

Adams, J. M. 1983. Hydrogen atom positions in kaolinite by neutron profile refinement. *Clays & Clay Miner.* **31**: 352–356.

Allegra, G. 1964. The calculation of the intensity of X-rays diffracted by monodimensionally disordered structures. *Acta Crystallog.* **17**: 579–586.

Bailey, S. W. 1963. Polymorphism of the kaolin minerals. *Am. Miner.* **48**: 1186–1209.

Bailey, S. W. 1980. Structures of layer silicates. In *Crystal Structures of Clay Minerals and their X-ray Identification.* G. W. Brindley and G. Brown, eds. London: Mineralogical Society, 1–124.

Bertaut, F. 1952. L'energie electrostatique de reseaux ioniques. *J. Phys. Radium* **13**: 499–505.

Bish, D. L. 1993. Rietveld refinement of the kaolinite structure at 1.5 K. *Clays & Clay Miner.* **41**: 738–744.

Bish, D. L., and R. B. Von Dreele. 1989. Rietveld refinement of non-hydrogen atomic positions in kaolinite. *Clays & Clay Miner.* **37**: 289–296.

Bleam, W. F. 1993. Atomic theories of phyllosilicates: Quantum chemistry, statistical mechanics, electrostatic theory, and crystal chemistry. *Rev. Geophys.* **31**: 51–73.

Bookin, A. S., V. A. Drits, A. Plançon, and C. Tchoubar. 1989. Stacking faults in kaolin-group minerals in the light of real structural features. *Clays & Clay Miner.* **37**: 297–307.

Brindley, G. W. 1980. Order-disorder in clay mineral structures. In *Crystal Structures of Clay Minerals and their X-ray Identification.* G. W. Brindley and G. Brown, eds. London: Mineralogical Society, 125–196.

Brindley, G. W., C. C. Kao, J. L. Harrison, M. Lipsicas, and R. Raythatha. 1986. Relation between structural disorder and other characteristics of kaolinites and dickites. *Clays & Clay Miner.* **34**: 239–249.

Brindley, G. W., and K. Robinson. 1946. Randomness in the structures of kaolinitic clay minerals. *Trans. Faraday Soc.* **42B**: 198–205.

Catti, M. 1978. Electrostatic lattice energy in ionic crystals: Optimization of the convergence of Ewald series. *Acta Crystallog.* **A34**: 974–979.

Collins, D. R., and C. R. A. Catlow. 1991. Energy-minimized hydrogen-atom positions of kaolinite. *Acta Crystallog.* **B47**: 678–682.

Coulon, C. 1971. La genese du massif rhyolitique du Mont Traessu (Sardaigne Septentrionale): Evolution de son dynamisme volcanique. *Boll. Soc. Geol. Ital.* **90**: 73–90.

Cowley, J. M. 1976. Diffraction by crystals with planar faults. I. General theory. *Acta Crystallog.* **A32**: 83–87.

Drits, V. A., and C. Tchoubar. 1990. *X-ray Diffraction by Disordered Lamellar Structures.* Berlin: Springer-Verlag, 233–303.

Giese, R. F. 1982. Theoretical studies of the kaolin minerals: electrostatic calculations. *Bull. Minéral.* **105**: 417–424.

Giese, R. F. 1991. Kaolin minerals: Structures and stabilities. *Rev. Mineral.* **19**: 29–66.

Hendricks, S., and E. Teller. 1942. X-ray interference in partially ordered layer lattices. *J. Chem. Phys.* **10**: 147–167.

Hess, A.C., and V. R. Saunders. 1992. Periodic ab initio Hartree-Fock calculations of the low-symmetry mineral kaolinite. *J. Phys. Chem.* **96**: 4367–4374.

Kakinoki, J., and Y. Komura. 1965. Diffraction by a one dimensionally disordered crystal. I. The intensity equation. *Acta Crystallog.* **19**: 137–147.

Larson, A.C., and R. B. Von Dreele. 1993. *GSAS, General Structure Analysis System*; Document LAUR 86-748, Los Alamos National Laboratory, New Mexico.

Michalski, E. 1988. The diffraction of X-rays by close-packed polytypic crystals containing single stacking faults. *Acta Crystallog.* **A44**: 640–649.

Newnham, R. E. 1961. A refinement of the dickite structure and some remarks on polymorphism in kaolin minerals. *Miner. Mag.* **32**: 683–704.

Plançon, A. 1981. Diffraction by layer structures containing different kinds of layers and stacking faults. *J. Appl. Crystallog.* **14**: 300–304.

Plançon, A., R. F. Giese, and R. Snyder. 1988. The Hinckley index for kaolinites. *Clay Miner.* **23**: 249–260.

Plançon, A., R. F. Giese, R. Snyder, V. A. Drits, and A. S. Bookin. 1989. Stacking faults in the kaolin-group minerals: Defect structures of kaolinite. *Clays & Clay Miner.* **37**: 203–210.

Plançon, A., and C. Tchoubar. 1975. Étude des fautes d'empilement dans les kaolinites partiellement désordonnées. I. Modèle d'empilement ne comportant que des fautes de translation. *J. Appl. Crystallog.* **8**: 582–588.

Plançon, A., and C. Tchoubar. 1976. Étude des fautes d'empilement dans les kaolinites partiellement désordonnées. II. Modèle d'empilement ne comportant que des fautes par rotation. *J. Appl. Crystallog.* **9**: 279–285.

Plançon, A., and C. Tchoubar. 1977a. Determination of structural defects in phyllosilicates by X-ray powder diffraction—I. Principle of calculation of the diffraction phenomenon. *Clays & Clay Miner.* **25**: 430–435.

Plançon, A., and C. Tchoubar. 1977b. Determination of structural defects in phyllosilicates by X-ray powder diffraction—II. Nature and proportion of defects in natural kaolinites. *Clays & Clay Miner.* **25**: 436–450.

Plançon, A., and C. Zacharie. 1990. An expert system for the structural characterization of kaolinites. *Clay Miner.* **25**: 249–260.

Suitch, P. R., and R. A. Young. 1983. Atom positions in highly ordered kaolinite. *Clays & Clay Miner.* **31**: 357–366.

Tchoubar, C., A. Plançon, J. Ben Brahim, C. Clinard, and C. Sow. 1982. Caractéristiques structurales des kaolinites désordonnées. *Bull. Mineral.* **105**: 477–491.

Thompson, J. G., and R. L. Withers. 1987. A transmission electron microscopy contribution to the structure of kaolinite. *Clays & Clay Miner.* **35**: 237–239.

Treacy, M. M., J. M. Newsam, and M. W. Deem. 1991. A general recursion method for calculating diffracted intensities from crystals containing planar faults. *Proc. R. Soc. Lond.* **433**: 499–520.

Van Olphen, H., and J. J. Fripiat. 1979. *Data Handbook for Clay Minerals and Other Non-Metallic Minerals.* Oxford: Pergamon Press, 71–82.

Young, R. A., and A. W. Hewat. 1988. Verification of the triclinic crystal structure of kaolinite. *Clays & Clay Miner.* **36**: 225–232.

(Received 22 November 1993; accepted 9 January 1994; Ms. 2441)